PHYSICAL REVIEW B VOLUME 20, NUMBER 2 15 JULY 1979

First- and second-order Raman scattering from finite-size crystals of graphite

R. J. Nemanich
Xerox Palo Alto Research Center, Palo Alto, California 94304

S. A. Solin
Department of Physics and The James Franck Institute, University of Chicago, Chicago, Illinois 60637

(Received 11 December 1978)

First- and second-order Raman scattering from graphite has been studied. The second-order spectra of single crystals and of highly oriented pyrolytic graphite are continuous and exhibit several well-defined bands which can be attributed to features in the density of vibrational states as determined from current lattice-dynamics models. The density of states deduced from the lattice-dynamics model of Nicklow, Wakabayashi, and Smith provides the best replication of the second-order Raman spectrum, but is nevertheless somewhat deficient in this regard, and in need of improvement. The dependence of the first- and second-order graphite Raman spectra on crystallite size has also been studied for a series of samples with typical dimensions L_c and L_a as small as 30 Å. With decreasing crystal size the features in the second-order spectrum broaden noticeably and additional broad features appear in both the first- and second-order spectra. The additional first- and second-order features are also attributed to structure in the vibrational density of states and arise from the wave-vector selection-rule relaxation that results from finite-crystal-size effects. Evidence is presented to demonstrate that the above described spectral features are intrinsic and not associated with impurity excitations.

I. INTRODUCTION

The bonding in graphite exhibits one of the largest anisotropies of any solid. Moreover the nearest-neighbor C-C bonding in graphite is considerably stronger than the C-C bond in diamond.[1] In contrast, the bonding between the planes is very weak and exhibits a Van der Waals character.[1] The very weak and very strong bonding in graphite will yield both unusually low- and high-frequency contributions to the lattice vibration spectrum.

The technique of choice for the study of the lattice dynamics of crystals has been neutron scattering. From a neutron scattering study of oriented single crystals one can in principle establish the complete phonon dispersion curves of the sample being examined.[2] In practice, however, neutron scattering suffers from several limitations. For instance, large single crystals are required. Since the available flux of slow neutrons with high energy, e.g., >500 cm^{-1} is minimal, that region of the phonon dispersion curves is difficult if not impossible to explore.[2] Also, the flux limitation reduces the accuracy of the neutron measurements to $\sim\pm5$ cm^{-1}. Finally, an intrinsic limitation of the neutron technique is its inability to provide crucial symmetry information on the vibrational excitations at key points in the Brillouin zone. Thus, though certainly necessary to an accurate understanding of the lattice dynamics of a crystal, it is clear that neutron scattering results may be insufficient. In such a case, second-order Raman spectroscopy can be a useful probe of the phonon properties.

The second-order Raman scattering is due to two-phonon states.[3] The scattering from large single crystals must satisfy wave-vector selection rules as does first-order Raman scattering. For second-order scattering, then, the sum of the phonon wave vectors must be equal to the wave vector transferred in the light scattering event. Since for visible exciting radiation the light scattering wave vector is ~1/1000 of that of the zone-boundary phonons, the two-phonon states sampled by second-order scattering have essentially equal and opposite wave vectors. If the two-phonon state is formed from phonons belonging to the same branch of the phonon dispersion curves and which have equal energy, that state is called an overtone. If the two-phonon state represents the sum or difference of two phonons with unequal energy the state is termed a combination. Therefore, because of the wave-vector conservation requirement, the spectrum of overtone states represents the density of one-phonon states convolved with the Raman matrix element, but the frequency scale is twice that of the one-phonon density-of-states spectrum. In contrast, the combination spectrum, of course, shows additional peaks not observed in the one-phonon density of states.

One of the most successful applications of second-order Raman scattering has been the study of diamond.[4,5] For this cubic crystalline form of carbon it was possible to establish accurate (±1 cm^{-1}) phonon energies and symmetries for many phonon branches at all high-symmetry points in

the Brillouin zone.[5] In addition an interesting anomalous feature was observed at the highest frequency of the second-order Raman spectra. This feature was attributed by Cohen and Ruvalds[6] to a two-phonon bound state, but this interpretation has been the subject of considerable recent controversy.[7-9] Subsequent similar second-order Raman studies of silicon and germanium also proved to be quite fruitful, although no anomalous "bound-state"-like feature was observed in those materials.[7,10]

If our understanding of diamond, silicon, and germanium, all extensively studied materials, could be enhanced by a second-order Raman study, then, such a study is even more appropriate to graphite. More importantly, the lattice dynamics of graphite, a prototypical lamellar compound, are not well understood. This lack of understanding persists even though neutron scattering studies of the low-energy (<500 cm^{-1}) dispersion curves have been carried out.[11,12] In addition, during the past several years, there have been many lattice-dynamics models which address the experimental neutron data.[12-16] Yet the theoretical models, several of which "fit" the neutron data, yield conflicting results in the high-frequency region. Moreover, given the lack of availability of large graphite single crystals and the high energy of the optical vibrations, there is little likelihood that the neutron scattering results will be significantly improved upon in the near future.

The limitation on available size of graphite crystals can be used to transform a vice into a virtue since it is possible to prepare graphite crystallites with typical dimensions ranging between 3 μm and 16 Å. With such crystallites one can in principle study the effects of finite crystal size on both the radiation-matter interaction and on the phonons themselves. In particular, the continuous relaxation of the wave-vector selection rules which are in principle appropriate only to infinite crystals can be probed with light scattering techniques.

The first Raman scattering studies of graphite were carried out by Tuinstra and Koenig.[17] These authors studied first-order scattering as a function of crystallite size and devised an empirical relation between the particle size and the relative intensity of a pair of first-order Raman bands. Subsequently Brillson *et al.*[18] studied the infrared reflectivity and polarized first-order scattering from the basal plane of graphite single crystals. The infrared measurements have been recently extended to include reflectivity from a face perpendicular to the basal planes.[19] In a previous study, we reported the second-order spectrum of graphite single crystals.[20] The focus of that preliminary report, however, was a very sharp, high-energy feature at 3248 cm^{-1} which was in some ways similar to the anomalous second-order feature of diamond and the presence of which had significant consequences for any lattice-dynamics model of graphite. Subsequently several authors have examined the first- and second-order Raman spectra of various forms of graphite,[21-23] including graphitizable carbon, coal, and coke,[24] as well as radiation-damaged material.[25,26] However, these studies have been primarily empirical and have focused on the growth and decay of particular spectral bands with sample history.

In this paper, we shall report second-order Raman scattering results from graphite samples which contain crystals of macroscopic to microscopic dimensions. Our results will be employed to refine and perfect the lattice-dynamics models of graphite, and we will interpret in a natural way unusual features of the second-order spectrum.

II. EXPERIMENTAL

Raman spectra were obtained from several different samples which included single crystals, highly oriented pyrolytic graphite (HOPG), glassy carbon, pressed carbon rods, and carbon powders. Polarized Raman measurements were performed in both the Brewster angle backscattering and true backscattering configuration using a cylindrically focused 4880-Å Ar-ion laser incident beam. The scattered light was dispersed with a Jarrel-Ash model 25-100 double monochromator equipped with Jobin-Yvon holographic gratings. In both scattering configurations the polarization measurements were made with the incident beam polarized either parallel (H) or perpendicular (V) to the scattering plane while the scattered beam was always analyzed parallel to the scattering plane. In the brewster angle configuration the scattering plane is that plane defined by the wave vectors of the incident and scattered photons.

To assure that the spectra obtained were intrinsic and free from impurity modes the HOPG sample was heated to ~1000 K for several hours under flowing He gas. In addition, all spectra were recorded with either a flow of helium gas on the sample or with the sample in a helium atmosphere in a sealed container.

III. RESULTS AND DISCUSSION

A. Crystalline graphite

There have been several ir[18,19] and first-order Raman studies[17,20,27,28] of graphite that have accurately determined the zone-center mode frequencies. The zone-center optic modes can be decomposed into the following irreducible repre-

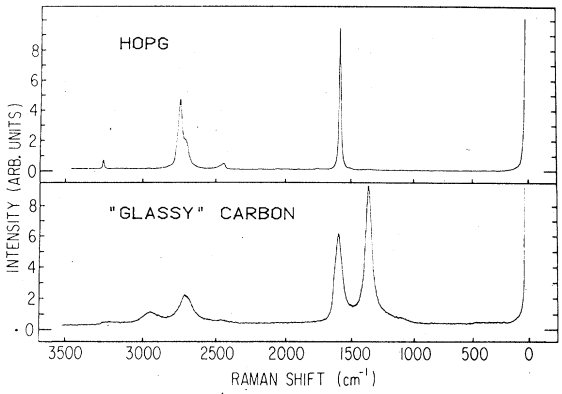

FIG. 1. First- and second-order Raman spectra of highly oriented pyrolytic graphite (HOPG) and "glassy" carbon. The spectra were recorded with a spectral slit width of ~10 cm^{-1}. For this figure and Figs. 8–11, the abscissas, while marked in cm^{-1}, are, however, linear in wavelength.

sentations[15]:

$$\Gamma = A_{2u} + 2B_{2g} + E_{1u} + 2E_{2g} . \quad (1)$$

The A_{2u} and E_{1u} modes are ir active and have been observed at 867 and 1588 cm^{-1}, respectively.[19] The E_{2g} modes are Raman active and have been observed at 42 and 1581 cm^{-1}.[28] The B_{2g} modes are optically inactive, however, one has been observed by neutron scattering at 127 cm^{-1} (Refs. 11 and 12) and the other will occur at a frequency near that of the A_{2u} (867 cm^{-1}). The E-symmetry modes exhibit "in-plane" atomic displacements while the A and B symmetry modes have "out-of-plane" displacements.[28]

In order to relate the first- and second-order Raman features of graphite the full Raman spectrum is shown in Fig. 1. The strong sharp feature at 1581 cm^{-1} is the high-frequency E_{2g} first-order mode. The low-frequency E_{2g} mode which occurs at 42 cm^{-1} is the interplanar "rigid-layer shear" mode and is only obtained with special techniques. The continuum scattering from 2200 to 3250 cm^{-1} represents the second-order features that are analyzed here. The second-order spectrum exhibits three distinct groups of bands. The spectrum is dominated by the strong features near 2710 cm^{-1}, and two weaker features are observed at ~2450 and ~3250 cm^{-1}.

Previously the validity of lattice-dynamics calculations of graphite has been tested by comparing the phonon dispersion curves, elastic constants, or specific-heat data deduced from them with experimental results. None of these tests have proven to be sensitive to the nature of the higher-frequency modes. The several recent full lattice-dynamics calculations of graphite can essentially be divided into two groups: those employing a Born–von Kármán model[12-16] and those employing a valence-force-field model.[29,30] Nicklow, Wakabayashi, and Smith[12] (NWS) proposed a model which used pairwise axially symmetric interactions to fit their neutron data. The model included interactions to fourth nearest neighbors: three "in-plane" neighbors and the nearest neighbor in adjacent planes. Recently Nicholson and Bacon[16] have extended the model of NWS to include axially symmetric pairwise interactions to fifth neighbors and three many-body valence force interactions. With this model the elastic constants could be fit without imposing restrictions that would lead to finite pressure at equilibrium as does the NWS model. Ahmadieh and Rafizadeh[13] and more completely Rafizadeh[14] have employed Lennard-Jones and Van der Waals potentials to describe the pairwise interactions also to fifth neighbors. They fit the zone-center frequencies to the observed vibrations of benzene and allowed other parameters to vary to provide a best fit to the neutron data. The results of the study of Nicholson and Bacon and the best fit obtained by Rafizadeh were very similar to the NWS results especially for modes with "in-plane" atomic displacements. The major difference was in the zone-center frequencies of the A_{2u} "out-of-plane" mode and here no model was consistent with the recently reported value.[19] It should also be noted that the inclusion of fifth-neighbor forces causes modes to exhibit mixed "in-plane" and "out-of-plane" character for some points in the Brillouin zone.[16] But because the forces are small they will not severely effect the high-frequency modes. Bridging the difference between valence force and Born–von Kármán models, Mani and Ramani[15] have used valence forces of the naphthalene molecule to arrive at values of several of the general tensor force constants. There has been a recent objection to their formalism,[16] and we find that their results are inconsistent with both the highest-frequency second-order feature at ~3248 cm^{-1} and the ir-active A_{2u} mode.

There have been two recent lattice-dynamics studies of graphite which directly employed valence-force-field models. Yoshimori and Kitano[29] used analytical techniques to calculate the vibrational density of states and more recently Young and Koppel[30] (YK) used more exact computer methods to carry out the calculation. Thus, in the following, we will focus on comparing the second-order Raman spectra to the results of NWS and YK because these calculations are typical and because each has been used to generate a vibrational density of states.

Before proceeding with a comparison of the density of vibrational states and second-order spec-

tra, several points must be considered. While second-order Raman spectra can reflect both overtone and combination vibrational states, previous experiments on Si,[7] Ge,[10] and diamond[5] indicate that the spectrum is often dominated by overtone states. This conclusion was obtained by comparison of second-order spectra to density of states determined from neutron scattering measurements. In addition, since overtone levels always contain an A_1 symmetry character (the product of any representation with itself always contains the identity),[31] these levels would be expected to contain a contribution which exhibits polarization characteristics typical of an A_1 mode, namely, to be stronger in configurations which measure the diagonal components of the Raman tensor. As is evident in Fig. 2, the entire spectrum from 2300 to 3250 cm^{-1} is uniformly and strongly polarized with respect to the first-order peak at 1581 cm^{-1}. Therefore, we assert that the spectrum is indeed dominated by overtone states.

In addition to the above assertion, it is also probable that none of the features of the second-order spectrum from 2300 to 3300 cm^{-1} arise from overtones of modes with "out-of-plane" atomic displacements. While both the NWS and YK models show contributions in this region, recent ir reflectivity measurements[19] have indicated that the A_{2u} zone-center, "out-of-plane" mode occurs at ~867 cm^{-1}. This mode is essentially degenerate with the highest-frequency zone-center B_{2g} mode. Since both the NWS and YK models show these modes to be the highest-frequency "out-of-plane" modes, the features of the second-order spectrum of graphite from 2300 to 3300 cm^{-1} can be analyzed only in terms of overtones of "in-plane" modes.

The second-order Raman spectra of graphite is compared to the calculated density of states and the two-phonon combination and overtone spectrum of "in-plane" modes obtained from the NWS model in Fig. 3. The NWS model calculation has been modified slightly to obtain the observed value for the high-frequency E_{2g} "in-plane" vibration (which we find at 1581 ± 1 cm^{-1}). It is evident that the observed Raman spectrum contains significantly fewer features than the total spectrum (combinations plus overtones). This supports the argument that the second-order Raman spectrum is composed predominantly of overtone derived modes.

The density of states were obtained by solving the dynamical matrix at 87 000 random points in an irreducible section of the Brillouin zone. While the NWS calculation does not yield an exceptional fit to the observed spectrum, several identifications can be made. Three strong features are shown in both the second-order Raman spectrum and the NWS calculation. Comparison of the calculated density of states with the calculated phonon dispersion curves (shown in Fig. 4) serves to show the critical points and the k-space regions which are associated with the peaks in the density of states. Because there is little dispersion of

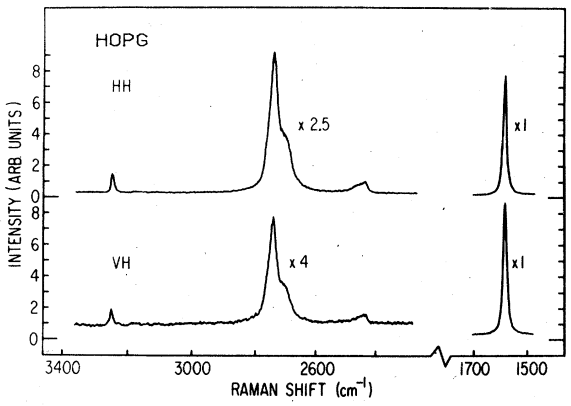

FIG. 2. Polarized first- and second-order Raman spectra of highly oriented pyrolytic graphite obtained using a Brewster angle backscatter configuration. The spectral intensities were normalized to account for the different reflectivities of the two polarization configurations.

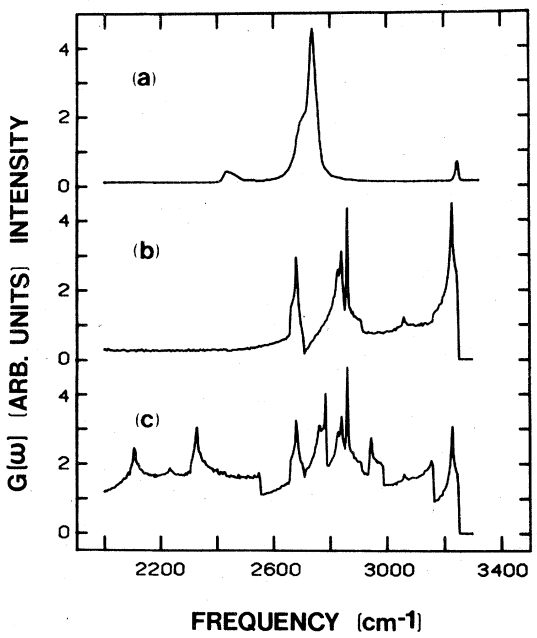

FIG. 3. Second-order Raman spectrum of highly oriented pyrolytic graphite (a) is compared with the "in-plane" one-phonon (b) and two-phonon (c) density of states obtained using the NWS model. The frequency scale of the one-phonon density of states has been multiplied by 2.

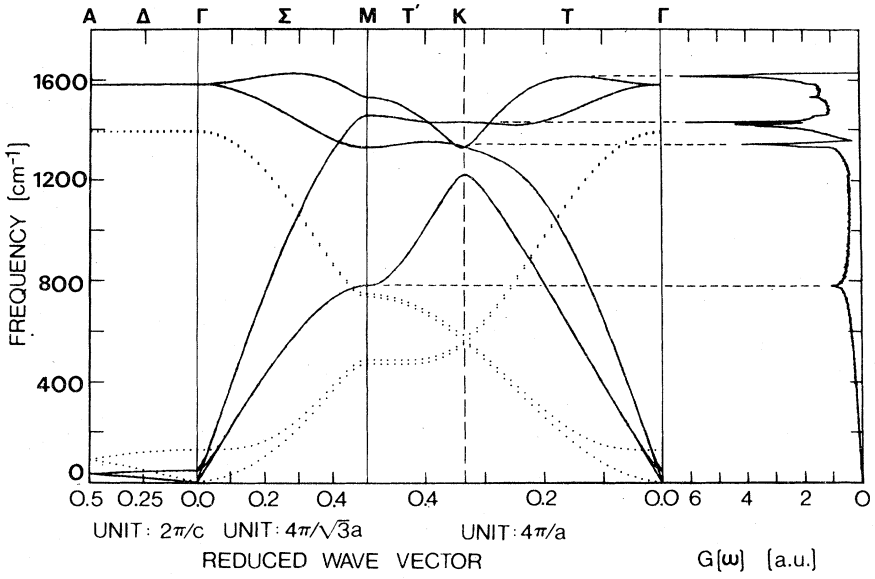

FIG. 4. Phonon dispersion curves and the density of states, $G(\omega)$, with "in-plane" displacements obtained with the NWS model. The dotted lines in the dispersion curves represent modes with "out-of-plane" displacements. The NWS force constants have been modified slightly to account for the Raman mode at 1581 cm^{-1}. The dashed horizontal lines are to show the k-space regions which contribute to the strong peaks in the density of states.

modes propagating perpendicular to the basal planes, the high-frequency region is characteristic of an ideal two-dimensional system. Therefore, "saddle"-type critical points in the phonon dispersion curves will yield logarithmic singularities in the density of states.[32] With respect to the graphite lattice, flatness of the phonon dispersion curves at the zone boundary (from M to K) will yield "saddle"-type critical points and thus strong features in the density of states. Consequently the flat curves at ~1340 and 1470 cm^{-1} along T' from K to M yield saddle points and hence the corresponding peaks in the phonon density of states of the NWS model. The peaks can then be ascribed to phonons with wave vector in the region of the corresponding critical point. In contrast, the highest-frequency strong feature in the density of states does not arise from modes along K to M, but instead is due to the flat maximum of the highest branches along Σ and T. It is this feature in the density of states that is a manifestation of the large second-neighbor forces employed in the NWS model.

To explore the nature of the observed 3248-cm^{-1} feature, we have calculated the phonon dispersion curves and density of states using several values of the second-neighbor force constants. The results of this calculation are shown in Fig. 5. Reducing the second-neighbor force constants does not affect the zone-center frequencies. However, when those force constants are reduced to 60% of the value used by NWS the maximum phonon frequency occurs at Γ rather than along T. This change causes the peak at the high end of the

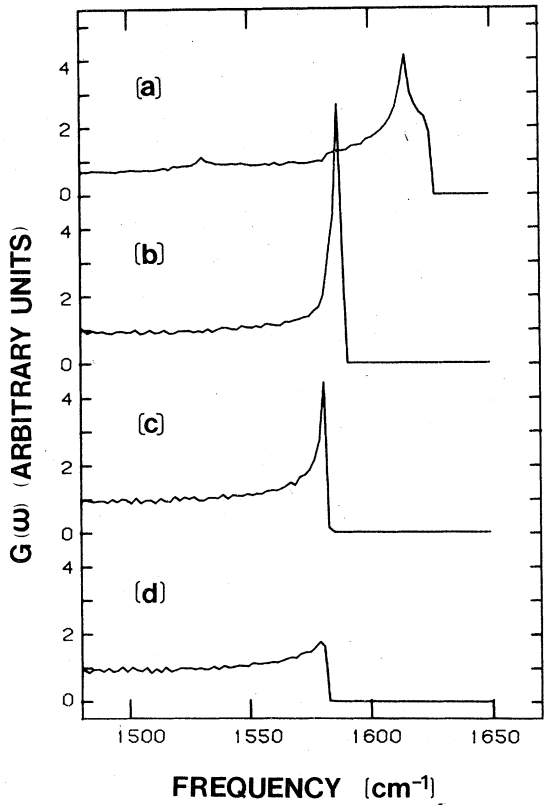

FIG. 5. High-frequency "in-plane" density of states obtained from the NWS model using several values of the second-neighbor force constants. The trace labeled (a) has the value used in the NWS calculation while (b), (c), and (d) are, respectively, 0.75, 0.60, and 0.50 of the original value.

phonon spectrum to shift from ~1620 to 1581 cm^{-1}. As the force constants are reduced further the peak decreases in intensity with respect to the background. We have carried out this exercise because an upward curvature of the highest Σ and T branches from Γ is unusual for covalently bonded materials. However, a sharp feature observed at the maximum frequency of the second-order spectrum of diamond has been attributed to either similar upward curvatures,[7,9] matrix element effects,[8] or a two-phonon bound state.[6] In the case of graphite, whether matrix effects or two phonon interactions are important, the large shift from 1581×2 to 1624×2 cm^{-1} observed here indicates that the unusual upward curvature of the phonon dispersion curves does indeed occur.

Consider now the YK model. This model as noted exhibits several deficiencies. The value predicted for the highest-frequency "in-plane" mode is 1688 cm^{-1} since the YK calculation was made before Raman and ir measurements indicated a value of ~1585 cm^{-1}. More seriously, there are no forces to give rise to the low-frequency "shear-type" rigid-layer modes or the small splitting of the E_{1u} and E_{2g} high-frequency modes. However, since the splitting is very small this will not significantly affect the density of states in the higher-frequency regions. More recently Tuinstra and Koenig[17]

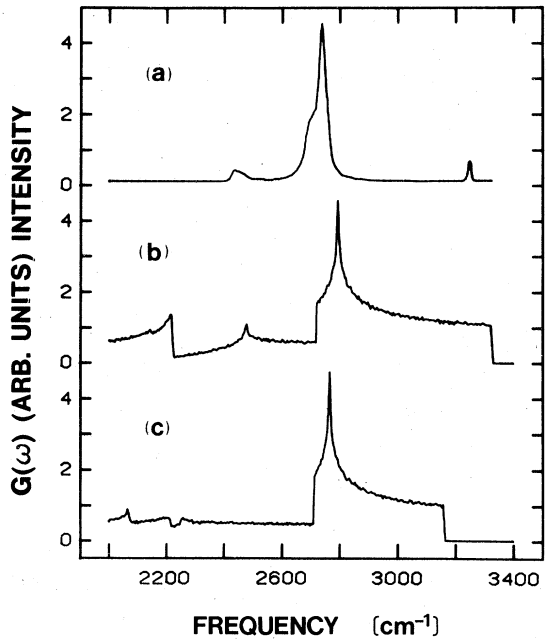

FIG. 6. Second-order Raman spectrum of HOPG (a) is compared with the "in-plane" one-phonon density of states of the YK model. Curve (b) is the result obtained using the YK force constants, and curve (c) is obtained using the TK force constants. The frequency scale of the one-phonon density of states has been multiplied by 2.

(TK) have suggested different bond-stretching and bond-bending force constants to obtain a zone-center frequency consistent with their Raman results. We have repeated the density-of-states calculation of the YK model using the force constants derived by both YK and TK. The "in-plane" density of states of these two cases of the YK model are compared with the second-order Raman spectrum in Fig. 6. The spectra obtained from both force-constant models are dominated by a single peak near 1400 cm^{-1}. As in the case of the NWS model, the features in this frequency region are due to critical points which arise from the flatness of the phonon dispersion curves along T' from K to M. This is illustrated in Fig. 7 where the YK density of states is compared with the corresponding phonon dispersion curves. In addition to the strong features, the model using the YK force constants yields weak features at ~1250 and ~1100 cm^{-1}. The ~1100-cm^{-1} feature has contributions due to the intersection of the acoustic and optic modes near the zone boundary. The corresponding features in the density of states in the TK model are much weaker and occur at a lower frequency. The absence of a sharp peak at the uppermost frequency in both density-of-states spectra is a manifestation of the fact that the highest-frequency mode is at Γ. We found that no variation of the bond stretching, k_r, and bond bending, k_θ, valence forces using the YK model could rectify this situation. Therefore additional valence forces are necessary to cause the upward bending of the phonon curves from Γ.

While neither the NWS nor YK model yields a

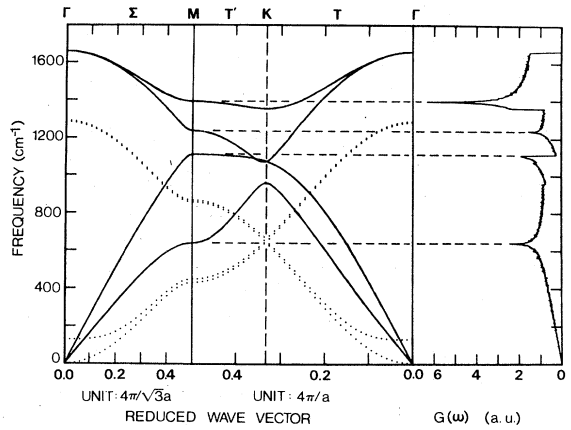

FIG. 7. Phonon dispersion curves and the density of states with "in-plane" displacements obtained with the YK model and the YK force constants. The dotted lines indicate modes with "out-of-plane" displacements and the horizontal dashed lines are to show the k-space regions which contribute to the strong peaks in the density of states.

density of states which agrees well with the observed second-order spectrum, the sharp features which occur in both calculations and the observed second-order spectrum seem to indicate the nature of the three main features observed experimentally. The strongest feature in the second-order spectrum at 2×1355 cm^{-1} is probably due to flatness of several branches between K and M. The step rise feature at ~2450 cm^{-1} also appears to arise from phonons in this same k-space region. An unusual aspect of the phonon dispersion curves shown in Fig. 4 is that the acoustic and low-frequency optic "in-plane" modes intersect the high-frequency "in-plane" modes near the zone boundary. In the NWS model this intersection is at ~1340 cm^{-1}. The peak in the NWS density of states at ~1340 is the one we have associated with the 2450-cm^{-1} (or 2×1225-cm^{-1}) band. Hence this feature takes on additional importance since it represents the intersection of the low-frequency and high-frequency "in-plane" modes. The highest-frequency feature in the second-order scattering at 3248 cm^{-1} is then attributed to scattering from the highest-frequency portions of the Σ and T branches. The frequency of the observed mode (3248 cm^{-1}) is almost exactly that predicted from the NWS model (2×1618 cm^{-1}). It seems reasonable to assume, then, that the scattering is due to critical points from flat maxima along Σ and T. This implies that the appropriate k-space region is not at the zone boundary. The NWS model shows, also, that the 3248-cm^{-1} peak is the strongest in the density-of-states spectrum, yet the observed intensity is significantly less than the intensity of the ~2700-cm^{-1} (2×1350-cm^{-1}) peak. This is probably due to matrix element effects because the mode arises from scattering at k-space points of lower symmetry.

B. Microcrystalline graphite

One of the most unusual properties of graphite is that the Raman spectrum of microcrystalline material shows additional lines that are not observed in large single crystals.[17,33] In Fig. 1 the full first-order spectrum of vitreous carbon is compared with that of single-crystal graphite, and the additional features are clearly displayed. In addition, the first- and second-order Raman spectrum of several samples with varying crystalline domain sizes are shown in Figs. 8 and 9. It is interesting that the strongest feature at 1355 cm^{-1} in the spectrum of "glassy" carbon is not observed in the spectra of large crystals. It was found that the relative intensity of the 1355-cm^{-1} mode with respect to the 1581-cm^{-1} mode varies as the inverse of the crystal planar domain size, L_a.[17] We have used this result to determine the domain size

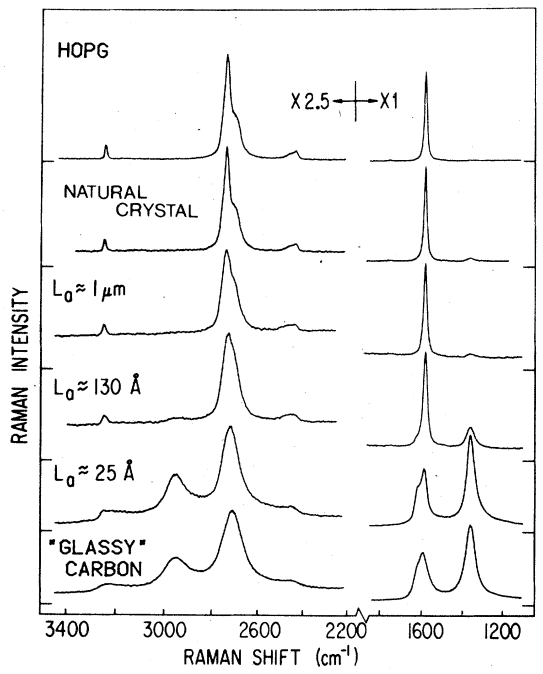

FIG. 8. First- and second-order Raman spectrum of several different forms of graphite. A spectral slit width of ~10 cm^{-1} was used.

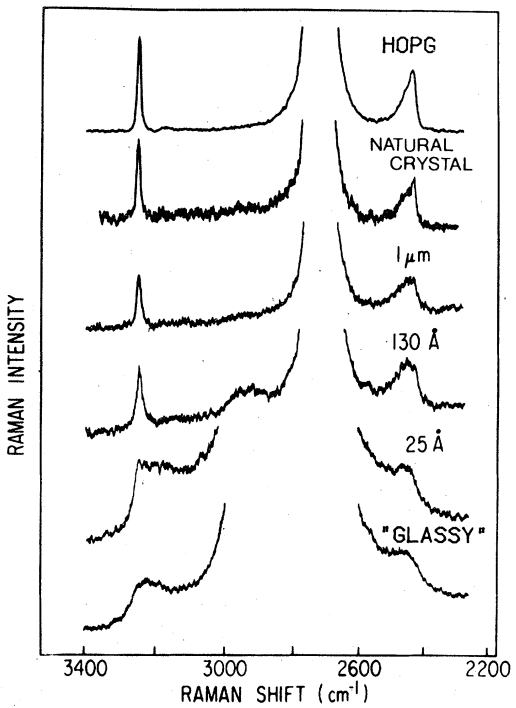

FIG. 9. Higher gain second-order Raman spectra of the same graphite samples used for Fig. 8.

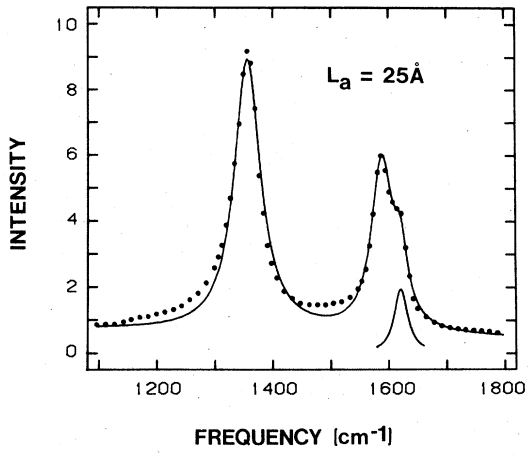

FIG. 10. Deconvolution of the peaks in the first-order Raman spectrum of microcrystalline graphite. The solid circles are the data and the solid line is a four Lorentzian fit. A broad Lorentzian was used to fit the background and the other three are centered at 1357, 1589, and 1621 cm^{-1}. The lower solid line shows the contribution due to the Lorentzian centered at 1621 cm^{-1}.

from the Raman spectra shown in Fig. 8. While the spectra of the samples with small L_a show the 1355-cm^{-1} line, all spectra display the usual first-order line at ~1580 cm^{-1}. The position of this mode is slightly dependent on domain size; shifting to higher frequency by ~10 cm^{-1} for the smallest L_a.[33] Closer examination of the ~1580-cm^{-1} mode in the samples with small L_a shows that it is actually a doublet. The higher-frequency component increases with decreasing L_a, exhibiting behavior similar to that of the 1355-cm^{-1} feature. A two-peak deconvolution of the doublet is shown in Fig. 10. It is evident that the higher-frequency component is sharp and occurs at ~1620 cm^{-1}.

The features observed below 1650 cm^{-1} fall in the first-order region, and given this, Tuinstra and Koenig have assigned the 1355-cm^{-1} mode to first-order scattering from a zone-boundary phonon activated by the disorder associated with finite crystallite size.[17] This assignment is corroborated by the observation of the strong feature at ~2710 cm^{-1} (i.e., ~2×1355 cm^{-1}) in the second-order Raman spectrum of large graphite single crystals. It should be mentioned that it is somewhat unusual to observe a zone-boundary feature in crystallites even as small as 30 Å. This is because the wave-vector uncertainty as determined by the uncertainty principle is $2\pi/L_a$, while the zone-boundary wave vector is $2\pi/a$, where a is the lattice constant. Thus even with the large uncertainty, because $L_a > a$ for all samples studied, it is difficult to account for the observation of the 1355-cm^{-1} line.

While the 1355-cm^{-1} mode has a counterpart in the second-order spectrum, if its presence results from small crystallite size, it might be expected that other features of the density of states are also reproduced. It is important to note that the ~1620-cm^{-1} feature also has a counterpart in the second-order spectrum of single-crystal graphite, namely, the 3248-cm^{-1} feature. In addition, as shown in Figs. 1 and 8, there is significant Raman intensity in the 1100–1300 cm^{-1} region that probably corresponds to the second-order feature at 2450 cm^{-1}. The differences in frequency between the observed first-order modes and half the frequency of the corresponding second-order feature could be due to matrix element effects or to the region of k space strongly sampled by the breakdown of wave-vector conservation. Second-order scattering will emphasize zone-boundary contributions while the disorder-induced scattering would emphasize the smaller k components. Hence, we assign these additional features in the first-order spectrum of microcrystalline samples to the corresponding features in the density of vibrational states.

The 1620-cm^{-1} line has recently been observed in neutron-irradiated pyrolitic graphite and in polycrystalline graphite by Maeta and Sato,[26] and they assigned the feature to the existence of C_2 molecules produced in the irradiation process. Because their spectra also show the ~1355-cm^{-1} mode, we suggest that the disorder due to the irradiation allows first-order scattering from the features in the density of states of the graphite network, and it is not necessary to invoke the presence of C_2 molecules. The Raman spectra reported by Tsu *et al.*[23] are similar to those reported here except they did not observe the second-order ~3248-cm^{-1} line. They suggested that the ~1620-cm^{-1} feature is due to a splitting of the doubly degenerate E_{2g} first-order line. In contrast we propose that the observation of the feature at ~3248 cm^{-1} is strong evidence for overtone scattering from the highest-frequency feature at ~1620 cm^{-1} in the density of states.

The second-order spectrum also exhibits an interesting dependence on crystallite size. As shown in Figs. 8 and 9, all the features broaden as the crystalline domain size is decreased. All structure at ~2700 cm^{-1} is lost and a single broad peak is observed. The features at ~2450 and ~3248 cm^{-1} actually obtain a step nature. While all features appear to broaden in a consistent manner, a new feature at ~2950 cm^{-1} grows with decreasing L_a. In order to ascertain whether these changes could be due to impurities, the Raman spectrum of a sample of polycrystalline graphite was examined before and after polishing. The polishing

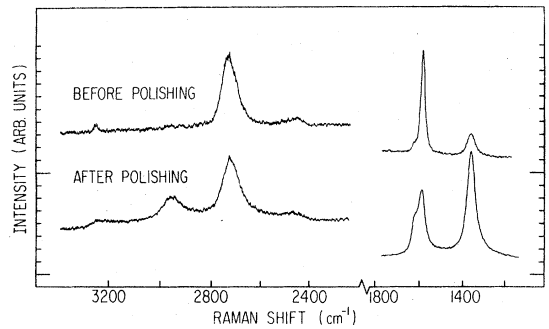

FIG. 11. The first- and second-order Raman spectra of polycrystalline graphite before and after polishing on ordinary paper.

was carried out by rubbing the surface on ordinary paper. The resultant spectra are shown in Fig. 11. The before and after polishing spectra indicate all the trends noted above. The same effect was observed using standard alumina polishing compounds. Thus it is unlikely that these effects could be attributed to impurities.

Second-order light scattering is similar to first-order scattering in that wave-vector conservation relations apply.[3] While in an infinite crystal the scattering involves two phonons with approximately opposite wave vectors, the microcrystalline domains will relax the wave-vector restriction in a way similar to that described for first-order scattering. Scattering can then occur for two phonons with different wave vectors where the wave-vector difference is again limited by the uncertainty relation. Therefore overtonelike scattering can occur from two phonons with slightly different energies because of the dispersion over the k-space region which is determined by the wave-vector uncertainty. Because of this, the sharp features of the density of states will be broadened in the light scattering spectrum of microcrystalline samples.

In addition to broadening, the wave-vector uncertainty can also serve to yield new features. Consider the case where two strong features in the density of states occur at different energies and arise from different wave-vector domains. For a large crystal wave-vector conservation precludes scattering in the second-order spectrum at a frequency equal to the sum of the frequencies. However, if this restriction is relaxed (as is the case for scattering from microcrystalline samples) a peak could occur at the sum of the frequencies of the two sharp features in the density of states. Of course matrix element effects must also be considered.

Thus it appears that the wave-vector uncertainty which arises from the microcrystalline domains is responsible for the effects observed in the second-order spectrum of graphite. The broadening of the three features which are sharp in the spectra of HOPG and natural crystal graphite is due to overtone-type scattering of two phonons with nearly equal energy. The origin of the peak at ~2950 is more complicated. We note that the sum of the frequencies of the 1355- and 1620-cm^{-1} modes is very near to the 2950-cm^{-1} value of the new feature in the second-order spectrum. We have argued above that these features were due to the strongest features in the density of states. It is, therefore, probable that the 2950-cm^{-1} feature arises from a combination of the strong density of states at ~1355 and ~1620 cm^{-1}. We note that the width of the 2950-cm^{-1} feature is approximately the same as that at 2700 cm^{-1}. Because the 1620-cm^{-1} component appears to be quite narrow, a convolution of the two features would yield a mode with the width approximately that of the broader feature. Thus the observed peak width of the ~2950-cm^{-1} feature is also consistent with the above explanation.

The interesting ~2950-cm^{-1} feature has also been reported by Wright *et al.*[25] and Tsu *et al.*[23] Wright *et al.* suggested that the mode was due to a combination of the zone-center 1580-cm^{-1} mode and the zone-boundary 1355-cm^{-1} mode. This is similar to the model posed above except we suggest that the high-frequency component is the highest-frequency feature in the density of states at ~1620 cm^{-1}. In contrast, Tsu *et al.* have suggested that the 2950-cm^{-1} feature is due to H impurities. We believe that the polishing and heating test rules out this possibility.

IV. SUMMARY

The second-order spectrum of single-crystal graphite shows several strong peaks in the frequency range of 2450–3250 cm^{-1} which have been ascribed to features in the density of vibrational states. While inelastic neutron scattering experiments have been previously reported on graphite, they only cover the frequency range of 0 to ~500 cm^{-1}. Thus the second-order Raman measurements which examine the one-phonon density of states in the 1200–1625-cm^{-1} region compliment the neutron measurements. In this paper we have compared the density of states deduced from several models of the graphite lattice dynamics with the observed Raman spectra. While some of the models showed similarities to the observed spectra, none yielded a quantitatively good description. Other properties that relate directly to the lattice dynamics are the ir reflectivity and elastic constants. These together with the Raman results

reported here should collectively provide sufficient constraints to allow an accurate rendition of the full lattice spectrum of graphite.

It is important to note that we have accounted for all the features observed in the polycrystalline and vitreous samples in terms of microcrystalline graphite structures only. The Raman spectrum of microcrystalline graphite shows several features not observed in single-crystal graphite. New peaks that occur at frequencies below 1650 cm^{-1} are also related to features in the density of states. Supportive of this contention is the fact that all new first-order features in microcrystalline graphite have counterparts in the second-order Raman spectrum of single-crystal graphite. The new modes are apparently due to the disorder associated with the microcrystalline domain sizes and the breakdown of the wave-vector selection rule. The entire second-order spectrum also shows changes with crystal size. The spectrum broadens consistently as the domain size decrease, and this affect is also attributed to the progressive relaxation of the wave-vector selection rule with decreasing domain size. A more unusual affect is the growth of a new peak at ~2950 cm^{-1} in the second-order spectrum. We ascribe this band to combination scattering associated with the two strongest features in the one-phonon density of states.

ACKNOWLEDGMENTS

We thank A. W. Moore for supplying the highly oriented pyrolytic graphite sample, and R. M. Martin for several helpful discussions. Research supported by the NSF Materials Research Laboratory of the University of Chicago and in part by the U.S. ERDA.

[1]A. R. Ubbelohode and F. A. Lewis, *Graphite and its Crystal Compounds* (Clarendon, Oxford, 1960).
[2]G. Dolling, in *Lattice Dynamics and Intermoleculor Forces* (Academic, New York, 1975).
[3]R. Loudon, Adv. Phys. 13, 423 (1964).
[4]R. S. Krishnan, Proc. Indian Acad. Sci. Sec. A 24, 45 (1946).
[5]S. A. Solin and A. K. Ramdas, Phys. Rev. B 1, 1687 (1970).
[6]M. H. Cohen and J. Ruvalds, Phys. Rev. Lett. 24, 1378 (1969).
[7]K. Uchinokura, T. Sekine, and E. Matsura, J. Phys. Chem. Solids 35, 171 (1974).
[8]S. Go, H. Bilz, and M. Cardona, Phys. Rev. Lett. 34, 580 (1975).
[9]R. Tubino and J. L. Birman, Phys. Rev. Lett. 35, 670 (1975).
[10]B. A. Weinstein and M. Cardona, Phys. Rev. B 7, 2545 (1973).
[11]G. Dolling and B. N. Brockhouse, Phys. Rev. 128, 1120 (1962).
[12]R. Nicklow, N. Wakabayashi, and H. G. Smith, Phys. Rev. B 5, 4951 (1972).
[13]A. A. Ahmadieh and H. A. Rafizadeh, Phys. Rev. B 7, 4527 (1973).
[14]H. A. Rafizadeh, Physica 74, 135 (1974).
[15]K. K. Mani and R. Ramani, Phys. Status Solidi B 61, 659 (1974).
[16]A. P. P. Nicholson and D. J. Bacon, J. Phys. C 10, 2295 (1977).
[17]F. Tuinstra and J. L. Koenig, J. Chem. Phys. 53, 1126 (1970).
[18]L. J. Brillson, E. Burstein, A. A. Maradudin, and T. Stark, in *Physics of Semimetals and Narrow Gap Semiconductors*, edited by Carter and Bate (Pergamon, New York, 1971), p. 187.
[19]R. J. Nemanich, G. Lucovsky, and S. A. Solin, Solid State Commun. 23, 117 (1977).
[20]R. J. Nemanich and S. A. Solin, Solid State Commun. 23, 417 (1977).
[21]M. I. Nathan, J. E. Smith, Jr., and K. N. Tu, J. Appl. Phys. 45, 2370 (1974).
[22]M. Nakamizo, R. Kammereck, and P. L. Walker, Jr., Carbon 12, 259 (1974).
[23] R. Tsu, J. H. Gonzalez, and I. G. Hernandez, Solid State Commun. 27, 507 (1978).
[24]R. Tsu, J. H. Gonzalez, I. G. Hernandez, and C. A. Luengo, Solid State Commun. 24, 809 (1977).
[25]R. B. Wright, R. Varma, and D. M. Gruen, J. Nucl. Mat. 63, 415 (1976).
[26]H. Maeta and Y. Sato, Solid State Commun. 23, 23 (1977).
[27]R. J. Nemanich, S. A. Solin, and D. Guerard, Phys. Rev. B 16, 2965 (1977).
[28]R. J. Nemanich, G. Lucovsky, and S. A. Solin, in *Proceedings of the International Conference on Lattice Dynamics*, edited by M. Balkanski (Flammarion, Paris, 1975), p. 619.
[29]A. Yoshimori and Y. Kitano, J. Phys. Soc. Jpn. 11, 352 (1956).
[30]J. A. Young and J. U. Koppel, J. Chem. Phys. 42, 357 (1965).
[31]E. B. Wilson, J. C. Decius, and P. C. Cross, *Molecular Vibrations* (McGraw-Hill, New York, 1955), p. 331.
[32]For a review, see A. A. Maradudin, E. W. Montroll, G. H. Weiss, and I. P. Ipatova, *Theory of Lattice Dynamics in Harmonic Approximation* (Academic, New York, 1971), p. 154.
[33]R. J. Nemanich, G. Lucovsky and S. A. Solin, Mater. Sci. Eng. 31, 157 (1977).